

Technical University of Denmark



## Influence of local wind speed and direction on wind power dynamics – Application to offshore very short-term forecasting

**Gallego, Cristobal; Pinson, Pierre; Madsen, Henrik; Costa, A.; Cuerva, A.**

*Published in:*  
Applied Energy

*Link to article, DOI:*  
[10.1016/j.apenergy.2011.04.051](https://doi.org/10.1016/j.apenergy.2011.04.051)

*Publication date:*  
2011

*Document Version*  
Early version, also known as pre-print

[Link back to DTU Orbit](#)

*Citation (APA):*  
Gallego, C., Pinson, P., Madsen, H., Costa, A., & Cuerva, A. (2011). Influence of local wind speed and direction on wind power dynamics – Application to offshore very short-term forecasting. *Applied Energy*, 88(11), 4087-4096. DOI: 10.1016/j.apenergy.2011.04.051

## DTU Library

Technical Information Center of Denmark

---

### General rights

Copyright and moral rights for the publications made accessible in the public portal are retained by the authors and/or other copyright owners and it is a condition of accessing publications that users recognise and abide by the legal requirements associated with these rights.

- Users may download and print one copy of any publication from the public portal for the purpose of private study or research.
- You may not further distribute the material or use it for any profit-making activity or commercial gain
- You may freely distribute the URL identifying the publication in the public portal

If you believe that this document breaches copyright please contact us providing details, and we will remove access to the work immediately and investigate your claim.

# Influence of local wind speed and direction on wind power dynamics - Application to offshore very short-term forecasting

C. Gallego<sup>a,\*</sup>, P. Pinson<sup>b</sup>, H. Madsen<sup>b</sup>, A. Costa<sup>a</sup>, A. Cuerva<sup>c</sup>

<sup>a</sup>*Wind Energy Unit, CIEMAT, Avd. Complutense 22, 28040. Madrid, Spain. Tel: +34 913466360*

<sup>b</sup>*DTU Informatics, Technical University of Denmark, Richard Petersens Plads 305, 2800 Kgs. Lyngby, Denmark.*

<sup>c</sup>*IDR/UPM, E.T.S.I.Aeronáuticos, Universidad Politécnica de Madrid, Pza. Cardenal Cisneros 3, 28040. Madrid, Spain*

---

## Abstract

Wind power time series usually show complex dynamics mainly due to non-linearities related to the wind physics and the power transformation process in wind farms. This article provides an approach to the incorporation of observed local variables (wind speed and direction) to model some of these effects by means of statistical models. To this end, a benchmarking between two different families of varying-coefficient models (regime-switching and conditional parametric models) is carried out. The case of the offshore wind farm of Horns Rev in Denmark has been considered. The analysis is focused on one-step ahead forecasting and a time series resolution of 10 minutes. It has been found that the local wind direction contributes to model some features of the prevailing winds, such as the impact of the wind direction on the wind variability, whereas the non-linearities related to the power transfor-

---

\*Corresponding author:

*Email address:* [cristobalj.gallego@ciemat.es](mailto:cristobalj.gallego@ciemat.es) (C. Gallego)

mation process can be introduced by considering the local wind speed. In both cases, conditional parametric models showed a better performance than the one achieved by the regime-switching strategy. The results attained reinforce the idea that each explanatory variable allows the modelling of different underlying effects in the dynamics of wind power time series.

*Keywords:* Energy systems modelling, Forecasting, Wind power, Offshore, Varying-coefficient

---

## 1. Introduction

The explosive growth of installed wind power over the last 10 years combined with the progressive liberalization of electrical markets have given rise to some new challenges related to wind energy [1]. Special attention has turned towards wind power forecasting, concerning the activity of two agents: wind power producers need to provide accurate information about their energy production in order to take part in the electrical market and the Transmission System Operators (TSO's) need to keep the stability of the electrical system also facing fluctuations on the generation side. In fact, when a certain penetration of wind generation is attained, uncertainties about the evolution of the wind may force the TSO to switch-off a certain number of wind farms, even when the resource is available. These facts represent a clear limitation for wind power penetration, specially considering the ambitious development plans of the offshore industry for the next years [2]. However, accurate forecasts for horizons varying from few minutes to several days could help to mitigate the impact of the inherent uncertainty of the wind. As a result, the last decade has witnessed a rapid growth in the field of short-term wind

18 power forecasting, for both statistical and physical approaches [3, 4, 5, 6, 7].

19 In this article we focus on the very-short term case, typically being based  
20 on a prediction horizon of some minutes to few hours. For such prediction  
21 horizons, it is generally accepted that statistical time series based models are  
22 more accurate than physical models, the latter ones being more appropriate  
23 for horizons beyond several hours [3, 5, 8]. The objective of statistical time  
24 series based models is to learn and replicate the dynamics shown by the tem-  
25 poral evolution of certain variables (such as the power output time series)  
26 under the hypothesis that these dynamics reflect different underlying effects  
27 of the wind power conversion process. Some of these effects would be at-  
28 mospheric processes occurring at different scales [9], the electrical conversion  
29 carried out by the wind turbine, the wake effect generated by nearby wind  
30 turbines, etc. [10, 11].

31 The present work aims to disentangle some of the effects mentioned above  
32 by means of a set of available local measurements and an appropriate sta-  
33 tistical model. Linear statistical models are characterized by their simplicity  
34 and reliability. Even though both wind speed and wind power time series  
35 show highly non-linear dynamics, several methodologies have been proposed  
36 based on a linear approach (see [12, 13, 14, 15, 16, 17, 18] among others).  
37 On the other hand, non-linear approaches are usually based on non paramet-  
38 ric models such as Artificial Neural Networks [19], which does not permit a  
39 clear interpretation of the underlying processes being modelled. We focus  
40 on a non-linear approach based on varying-coefficient models [20] by gen-  
41 eralising linear Autoregressive models (AR). The basic structure of an AR  
42 model considers the forecasted value as a linear combination of past values

43 by employing fixed weights (see Eq. 6). The main idea is to replace these  
44 constant parameters by functions that take into account local observations  
45 such as wind speed and direction. This allows the modelling of dependencies  
46 in the time series dynamics based on other explanatory variables in a simple  
47 way.

48 Regime-switching autoregressive models are a particular case of varying-  
49 coefficient models that consider AR coefficients as constant piece-wise func-  
50 tions. In this case, the considered time series is supposed to evolve shift-  
51 ing between clearly differentiated dynamics (called regimes). These kind of  
52 models give rise to a new problem because regimes have to be identified and  
53 delimited in some sense [21]. If the shift between regimes is modelled as a  
54 function of lagged values of a time series, the process is called observable.  
55 This is the case of Threshold Autoregressive Open Loop (TARSO) models  
56 [22, 23, 24]. A different approach is considered by Markov Switching Au-  
57 toregressive models (MSAR), where the current regime is a non-observable  
58 process following a first order Markov chain [25, 26, 27, 28, 29, 30].

59 On the other hand, Conditional Parametric Autoregressive models (CPARX)  
60 consider the AR coefficients as smooth functions of some explanatory vari-  
61 ables [31, 32, 33]. There exist several approaches to estimate these coefficient-  
62 functions (see [34] and references therein). For example, the locally weighted  
63 linear regression introduced by Cleveland and Devlin [35] was applied in the  
64 design of the Danish Wind Power Prediction Tool WPPT4 [36]. In that case,  
65 the AR coefficients were modelled as a function of the forecasted wind speed  
66 and direction provided by physical Numerical Weather Prediction (NWP)  
67 model.

68 To the authors' knowledge, there is relatively little research concerning  
69 regime-switching models and conditional parametric models that take into  
70 account on-line available data such as local wind speed and direction. Thus,  
71 in this article we propose a benchmark between the two mentioned families  
72 of models (regime-switching and conditional parametric models) in order to  
73 clarify how this information can be added so as to model specific features  
74 of the wind power time series dynamics. Three reference models are also  
75 considered: Persistence, linear AR and MSAR models. Table 1 summarizes  
76 different regime-switching and conditional parametric models reviewed in the  
77 literature, as well as those considered in this study.

78 The paper is structured as follows: In Section 2 a theoretical descrip-  
79 tion of the models considered in this article is presented. In Section 3 the  
80 database of the case study is described, the offshore wind farm of Horns Rev.  
81 The application of the models are detailed in Section 4, organized in four  
82 subsections:(i) Description of the reference models, (ii) Modelisation of the  
83 local wind direction influence, (iii) Modelisation of the local wind speed influ-  
84 ence and (iv) Combining the effects of both local wind speed and direction.  
85 Results are presented and discussed in Section 5. Finally, the main findings  
86 of the article are summarized in Section 6.

## 87 **2. Theoretical description of the models**

88 From now,  $\{y_t\}$ ,  $t = 1, \dots, N$  represents a discrete time series with  $N$   
89 observations of averaged wind power production.  $\{x_t\}$ ,  $x_t \in \mathbb{R}$ ,  $t = 1, \dots, N$   
90 is a discrete time series with  $N$  observations of a certain exogenous variable.  
91 Additionally,  $\mathcal{Y}_T$  and  $\mathcal{X}_T$  denote vectors gathering the first  $T$  values of the

92 corresponding time series, e.g.  $\mathcal{Y}_T = (y_1, \dots, y_T)$ .  $\{y_t\}$  is supposed to follow  
 93 a stochastic process like:

$$y_t = f(\mathcal{Y}_{t-k}, \mathcal{X}_{t-k}, \Theta) + \varepsilon_t \quad (1)$$

94  $f$  provides the deterministic component of  $y_t$  as a function of a certain  
 95 set of parameters  $\Theta$  and the available observations  $\mathcal{Y}_{t-k}$  and  $\mathcal{X}_{t-k}$ ,  $k$  being  
 96 the prediction horizon.  $\{\varepsilon_t\}$  is a white noise process, that represents the  
 97 noise of the stochastic process. The purpose of each model considered is  
 98 to determine a certain function  $\hat{f}$ , this function being a proposal for the  
 99 unknown deterministic component of the process. Nevertheless, there are  
 100 some considerations that establish a common framework for the development  
 101 of every model considered here. First, only the case of one-step ahead is  
 102 considered, thus,  $k = 1$ . Moreover, the white noise is assumed to follow a  
 103 centred Gaussian distribution with standard deviation  $\sigma$ , i.e.,  $\varepsilon_t \sim \mathcal{N}(0, \sigma^2)$ .  
 104 Hence, a certain model forecasts the value  $y_t$ , denoted with  $\hat{y}_t$ , as follows:

$$\hat{y}_t = E(y_t | \mathcal{Y}_{t-1}, \mathcal{X}_{t-1}, \Theta) = \hat{f}(\mathcal{Y}_{t-1}, \mathcal{X}_{t-1}, \Theta) \quad (2)$$

105 where  $E(a|b)$  represents the expectation of the statistical variable  $a$  given  $b$ .

106 In order to estimate the set of parameters of a statistical model,  $\Theta$ , the  
 107 minimisation problem given by Eq. (3) has to be considered along with a  
 108 score function. In this work we use the quadratic error function of Eq. (4)  
 109 evaluated over a set of historical data (training-set) with  $N_{train}$  samples.

$$\hat{\Theta} = \underset{\Theta}{\operatorname{argmin}} \mathcal{E}(\Theta) \quad (3)$$

$$\mathcal{E}(\Theta) = \sum_{t=p+1}^{N_{train}} (y_t - \hat{y}_t)^2 \quad (4)$$

110 In the following subsections, the linear reference models are described first  
 111 (Persistence and linear AR), then a non-linear reference model (the MSAR  
 112 model, a regime-switching model without exogenous variables) and finally,  
 113 TARSO and CPARX models, which comprise a set of varying-coefficient  
 114 models that take into account the local wind direction and the local wind  
 115 speed as explanatory variables.

116 *2.1. Linear reference models: Persistence and autoregressive*

117 Persistence is the most common reference forecasting method for predic-  
 118 tion horizons up to 4-6 hours, due to the characteristic time of changes in the  
 119 atmosphere [37]. A clear advantage of this model is that neither a parameter  
 120 estimation nor exogenous variables are needed. Persistence states that the  
 121 forecasted value at time  $t$  is the last available value:

$$\hat{y}_t = y_{t-1} \quad (5)$$

122 An  $AR(p)$  is an order- $p$  linear model that considers  $\hat{y}_t$  as a weighted sum  
 123 of the previous  $p$  observed values:

$$\hat{y}_t = \theta_0 + \sum_{i=1}^p \theta_i \cdot y_{t-i} \quad (6)$$

124 In this case, given a certain order  $p$ , the set of parameters  $\Theta$  gathers the  
 125  $p + 1$  AR coefficients. This set will be noted as  $\Theta_{AR(p)}$

$$\Theta_{AR(p)} = \{\theta_0, \theta_1, \dots, \theta_p\} \quad (7)$$



126 Since varying-coefficient models proposed in this article are obtained by  
127 generalising a linear AR model, comparison between them reveals the im-  
128 provement obtained just related to the consideration of changing regimes or  
129 smooth dependencies.

## 130 *2.2. Non-linear reference model: Markov-Switching Autoregressive Models*

131 The first generalisation of linear AR models considered are the MSAR  
132 models. These models assume that a time series evolves switching between  
133 different autoregressive dynamics (called regimes). The shift between regimes  
134 is considered as a non observable process, which means that it cannot be de-  
135 termined by lagged values of the time series. Pinson et al. [29] demonstrated  
136 that MSAR models provided better results than other regime-switching mod-  
137 els for two case studies of off-shore wind power forecasting, mainly because  
138 these models manage to capture more complex dynamics in regime-switching  
139 than when considering the regime as an observable process. Hence, MSAR  
140 models represent a suitable option to evaluate the improvement related to  
141 regime-switching hypothesis in the absence of exogenous variables. For this  
142 reason, MSAR models are here considered as the third reference model.

143 Let us consider that a time series evolves according to a certain num-  
144 ber,  $r$ , of different regimes. The current regime at time  $t$  is given by the  
145 discrete state variable  $s_t$ ,  $t = 1, \dots, N$ ,  $s \in \{1, \dots, r\}$ . The shift between  
146 regimes is governed by a first order Markov chain, hence the probability  
147  $p(s_t | \mathcal{S}_{t-1}, \mathcal{Y}_{t-1}) = p(s_t | s_{t-1})$ . These probabilities are collected in the so-  
148 called transition matrix  $P$ , where  $P_{ij} = p(s_t = j | s_{t-1} = i)$ . Since the process  
149 is considered unobservable,  $\{s_t\}$  is hidden and has to be inferred from avail-  
150 able data through the Hamilton filter introduced in Hamilton [38]. Each

151 regime  $j$ ,  $j = 1, \dots, r$ , is supposed to follow an  $\text{AR}(p)$  process with coefficients  
 152  $\Theta_{\text{AR}(p)}^{(j)} = \{\theta_0^{(j)}, \dots, \theta_p^{(j)}\}$  and standard deviation  $\sigma^{(j)}$ . The set of parameters of  
 153 the MSAR model,  $\Theta_{\text{MSAR}}$ , gathers the transition matrix, the AR coefficients  
 154 and the standard deviation for each regime:

$$\Theta_{\text{MSAR}} = \{P, \Theta_{\text{AR}(p)}^{(1)}, \dots, \Theta_{\text{AR}(p)}^{(r)}, \sigma^{(1)}, \dots, \sigma^{(r)}\} \quad (8)$$

155 As an example, Figure 1 illustrates the filtered probabilities of the current  
 156 regime along with the power output time series for a short window time. It  
 157 can be seen how the filtered probabilities balance depending on the level of  
 158 fluctuations. During periods with missing-data, the transition matrix deter-  
 159 mines a smooth exponential convergence to the so-called ergodic probabilities  
 160 (the probabilities of being in a certain regime at an arbitrary date).

161 MSAR models can be formulated in two different ways [39]: the Intercept-  
 162 Form (MSAR-IF, Eq. 9) and the Mean Adjusted Form (MSAR-MAF, Eq.  
 163 10).

$$y_{t,IF}^{(s_t)} = \theta_0^{(s_t)} + \sum_{i=1}^p \theta_i^{(s_t)} \cdot y_{t-i} + \varepsilon_t^{(s_t)} \quad (9)$$

$$y_{t,MAF}^{(s_t)} - \mu_0^{(s_t)} = \sum_{i=1}^p \phi_i^{(s_t)} \cdot (y_{t-i} - \mu_0^{(s_{t-i})}) + \varepsilon_t^{(s_t)} \quad (10)$$

164 When no regimes are considered, both forms are equivalent by considering  
 165  $\phi_i = \theta_i, \forall i > 0$  and  $\mu_0 = \theta_0 / (1 - \sum_{i=1}^p \theta_i)$ . Nevertheless, MSAR-IF and  
 166 MSAR-MAF model different underlying dynamics [39].

167 *2.3. TARSO models*

168 Open Loop Threshold Autoregressive models are a kind of regime-switching  
 169 model where the current regime  $s_t$  is assessed by a predefined function of the  
 170 available observations of exogenous variables,  $s_t = s_t(\mathcal{X}_{t-1})$ . Hence the pro-  
 171 cess is called observable. Usually, only a certain lag of  $x_t$  is considered,  
 172  $s_t = g(x_{t-lag})$ . In that case, regimes are settled by a certain number of  
 173 thresholds,  $l_0, l_1, l_2, \dots, l_r$ , that divide the space spanned by  $\{x_t\}$  in  $r$  subsets,  
 174 called  $S_j$ ,  $j = 1, \dots, r$  from now. Then,  $x_{t-lag} \in S_j \Leftrightarrow l_{j-1} \leq x_{t-lag} < l_j$ .

175 In this article only the previous lag of the exogenous variable is considered  
 176 in assessing regimes. An AR process is assumed in each regime. For the sake  
 177 of simplicity, all the AR processes will have the same order  $p$ . The model is  
 178 given by:

$$y_t = \theta_0^{(s_t)} + \sum_{i=1}^p \theta_i^{(s_t)} \cdot y_{t-i} + \varepsilon_t^{(s_t)} \quad (11)$$

$$s_t = \begin{cases} 1, & x_{t-1} \in S_1 \\ 2, & x_{t-1} \in S_2 \\ \dots & \\ r, & x_{t-1} \in S_r \end{cases}$$

179 With the mentioned hypothesis, the implementation of a TARSO model  
 180 gives rise to three questions: (i) what is the number,  $r$ , of regimes considered,  
 181 (ii) what is the optimal value for the set of thresholds  $\mathbf{l} = \{l_0, \dots, l_r\}$  and (iii)  
 182 what AR order  $p$  to choose.

183 Modelling a wind power time series with the described TARSO model

184 implies that the wind farm output has clearly differentiated dynamics de-  
 185 pending on the value of some observed variable. For example, in the case  
 186 of the wind direction ( $wd$ ), a different behaviour of the wind power time  
 187 series would be expected depending on the local wind direction observed at  
 188 the moment of making the forecasting,  $wd_{t-1}$ . If  $wd_{t-1}$  crosses one of the  
 189 thresholds given by  $\mathbf{l}$ , then there is an abrupt change on the AR process that  
 190 provides the forecast  $\hat{y}_t$ .

#### 191 2.4. CPARX Models

192 Conditional parametric models are characterized by a smooth dependence  
 193 of their coefficients with a certain variable. In particular, the CPARX models  
 194 generalize an AR model by letting the coefficients depend on available obser-  
 195 vations of exogenous variables,  $\theta_i = \theta_i(\mathcal{X}_{t-1})$ . As in the preceding case, only  
 196 the previous lag of the exogenous variable will be considered. The model is  
 197 given by:

$$y_t = \theta_0(x_{t-1}) + \sum_{i=1}^p \theta_i(x_{t-1}) \cdot y_{t-i} + \varepsilon_t \quad (12)$$

198 A central point is how to define the coefficient-functions  $\theta_i(x_{t-1})$ . They  
 199 can be estimated with non-parametric techniques from historical data or by  
 200 means of a parametric function [40, 41]. In this work, the latter case will be  
 201 considered.

202 Modelling a wind power time series with a CPARX model implies that  
 203 the wind farm output dynamic is expected to change smoothly depending  
 204 on the value of some observed variable  $x_{t-1}$ . For example, in the case of the  
 205 wind speed, ( $ws$ ), the observed local value  $ws_{t-1}$  fixes at each time step the

206 AR process (through the coefficient-functions  $\theta_i(ws_{t-1})$ ) that provides the  
207 forecast  $\hat{y}_t$ .

### 208 **3. Description of the data**

209 The data considered originates from the offshore wind farm located at  
210 Horns Rev, off the west coast of Denmark. This wind farm has a rated  
211 power of 160 MW. Measurements of wind power output, wind speed and  
212 direction are available for each wind turbine, with a one-second sample rate.  
213 10-minute resolution time series are derived by averaging raw data. At least  
214 75% of the data within an interval has to be considered as valid in order  
215 to consider the averaged value also valid. The averaging process assures  
216 that the fast fluctuations related to the turbulent nature of the wind have  
217 been filtered. The period considered ranges from 16th February 2005 to 31st  
218 January 2006, consisting of 50,400 data points with 8,790 missing data. The  
219 data-base has been divided into the following 3 sets:

- 220 · Training-set, from 16th February to 31st May 2005: the parameters  
221 of the models are estimated considering this data set by solving the  
222 minimisation problem given by Eq. (3).
- 223 · Validation-set, from 1st June to 31st August 2005: the forecasts pro-  
224 vided by the trained models are evaluated during this second period.  
225 By doing this, it is possible to assess the generalization capabilities  
226 of each model, which means that a certain model trained over a first  
227 period keeps its prediction performances over a different time period.

228 · Test-set, from 1st September 2005 to 31st January 2006: a benchmark  
229 analysis between validated models is carried out based on their fore-  
230 casting performance in this period.

231 It should be notice that the division of the data-set does not permit  
232 models to capture seasonalities during the training process, which covers  
233 almost four months. This seasonalities are expected to be present in wind  
234 power time series considering the seasonal variability of wind at Horns Rev  
235 observed in Vincent et al. [42]. However, it does not necessarily imply that  
236 the optimal models would dramatically change from one month to another.  
237 In any case, the optimisation of the models taking into account seasonal  
238 variations would require several years of data (not available for this work) and  
239 the implementation of models with time-varying parameters being adaptively  
240 estimated. In this regard, the implementation of adaptive MSAR models was  
241 addressed in [30].

#### 242 **4. Application of the models**

243 In this section, the implementation of the models considered in Section  
244 2 in the case of data described in Section 3 is presented. The section is  
245 divided in four subsection on different alternatives about the explanatory  
246 variables considered. Each model is trained with different structures (con-  
247 cerning for example the AR order and the definition of regimes). The optimal  
248 parametrisation of each model was chosen regarding the generalisation capa-  
249 bilities across the validation-set. The performance of the models is evaluated  
250 in terms of the Normalized Root Mean Square Error (*NRMSE*) and the  
251 percentage of Improvement Over Persistence (*IoP*), defined as follows:

$$NRMSE = \frac{1}{P_N} \cdot \sqrt{\sum_{t=p+1}^N \frac{(y_t - \hat{y}_t)^2}{N - p}} \quad (13)$$

$$IoP(\%) = 100 \cdot \frac{NRMSE_0 - NRMSE}{NRMSE_0} \quad (14)$$

252 where  $P_N$  is the rated power of the wind farm and  $NRMSE_0$  is the  $NRMSE$   
 253 obtained with Persistence . Both criteria are suggested in Madsen et al. [37],  
 254 which includes a broad overview of ways to evaluate wind power prediction  
 255 methods.

#### 256 4.1. Reference models

257 This subsection deals with the implementation of the reference models  
 258 described in subsections 2.1 (Persistence and linear AR) and 2.2 (MSAR  
 259 models). As previously mentioned, Persistence does not have free parameters  
 260 to be estimated. Thus, the performance of this model is evaluated in a  
 261 straightforward way. This is not the case for the linear AR models, since  
 262 the appropriate AR order  $p$  and the set of parameters  $\Theta_{AR(p)}$  need to be  
 263 estimated. For a given value of  $p$ ,  $\Theta_{AR(p)}$  is estimated by means of the Yule-  
 264 Walker equations (available in several works, e.g. [43]) over the training  
 265 period. Then, the evaluation of the trained models over the validation-set  
 266 allowed the optimal value of  $p = 3$  to be identified.

267 Next, both MSAR-IF and MSAR-MAF architectures are employed to  
 268 model the wind power time series of Horns Rev. In order to estimate  $\Theta_{MSAR}$ ,  
 269 the Expectation-Maximization algorithm introduced in Dempster et al. [44]  
 270 and further described in Hamilton [45] is applied (for further details, see [38,

271 46]). In the case of the MSAR-IF form, three regimes were identified with  
 272 the following set of parameters:

Regime	$\theta_0$	$\theta_1$	$\theta_2$	$\theta_3$	$\sigma$
$s_t = 1$	0.01	1.24	-0.47	0.19	0.0573
$s_t = 2$	0.04	1.21	-0.24	0.00	0.0004
$s_t = 3$	0.00	1.45	-0.50	0.04	0.0075

$$P = \begin{bmatrix} 0.77 & 0.02 & 0.21 \\ 0.11 & 0.73 & 0.16 \\ 0.27 & 0.03 & 0.70 \end{bmatrix}$$

273 On the other hand, the MSAR-MAF model identified the two following  
 274 regimes:

Regime	$\mu_0$	$\phi_1$	$\phi_2$	$\phi_3$	$\sigma$
$s_t = 1$	0.52	1.25	-0.46	0.18	0.0565
$s_t = 2$	0.53	1.38	-0.45	0.08	0.0121

$$P = \begin{bmatrix} 0.91 & 0.09 \\ 0.07 & 0.93 \end{bmatrix}$$

275 In both cases, the regimes were identified by sorting different levels of  
 276 fluctuations, i.e., different values for  $\sigma^{(i)}$ , the standard deviation of the noise.

#### 277 4.2. Modelling the influence of the local wind direction

278 In this subsection, the inclusion of the local wind direction into both  
 279 TARSO and CPARX models is detailed. In order to get some clues about



280 the dependence of wind power on wind direction, a preliminary analysis has  
 281 been carried out. This would eventually suggest restrictions to the design of  
 282 appropriate varying-coefficient models, e.g. the number of regimes and the  
 283 shape of the parameter functions. Then, both the TARSO( $wd$ ) model and  
 284 the CPARX( $wd$ ) model are implemented.

#### 285 4.2.1. Preliminary analysis

286 The central idea is to train a linear AR model over a subset of the training  
 287 data. The subset is given by the membership of the previous wind direction  
 288 lag to a certain sector over the wind rose. The set of AR coefficients,  $\Theta_{AR}$ ,  
 289 and the *NRMSE* obtained characterize the dynamic of the wind power output  
 290 related to this particular sector. Then, by sliding smoothly the orientation  
 291 of the sector and repeating the process, one observes the impact of wind  
 292 direction on wind power dynamics.

293 Let us consider a main direction  $\alpha_0$  and a sector width  $h$ . The AR( $p$ )  
 294 model for this sector is given by:

$$\begin{cases} \hat{y}_t = \theta_0 + \sum_{i=1}^p \theta_i \cdot y_{t-i} \\ \forall t : wd_{t-1} \in \alpha_0 \pm h/2 \end{cases}$$

295 The estimation of this model provides specific values for  $\Theta_{AR(p)}$  and  
 296 *NRMSE*, related to  $\alpha_0$ . Figure 2 illustrates the dependence of  $\alpha_0$  on  $\theta_{AR(p)}$   
 297 and the *NRMSE*, when considering the case for  $p = 2$  and  $h = 90^\circ$ . The  
 298 following conclusions were derived from the previous analysis, where the  
 299 considered values for  $p$  ranged from 1 to 5: (i) AR coefficients showed a  
 300 certain dependence on  $\alpha_0$  for any value of  $p$ . This dependence is smooth  
 301 sinus-shaped. (ii) The highest *NRMSE* (thus, the lowest predictability) is

302 related to 270°-310° directions. (iii) The relationship between the *NRMSE*  
 303 and  $\alpha_0$  shows a similar tendency in both the training-set and the validation-  
 304 set. Hence, the influence of the wind direction learnt from historical data  
 305 seems to be representative enough to model future behaviour.

#### 306 4.2.2. *TARSO models based on a wind direction criterion: TARSO(wd)*

307 The previous analysis highlights different predictability levels, depending  
 308 on the wind direction. Furthermore, there seems to be a high predictability  
 309 orientation (E-SE), a low one (W-NW) and intermediate transitions. This  
 310 fact suggests a low number of regimes to be considered a priori.

311 The TARSO model was introduced in Eq. (11). In this particular case,  
 312 regime thresholds  $\mathbf{l}$  will be related to wind direction sectors as follows: let  
 313 us consider a main direction  $\alpha_0$  and a certain width sector  $h$ . For the sake  
 314 of simplicity, the same  $h$  will be considered for every sector. The wind rose  
 315 can be split in  $r = 360^\circ/h$  sectors (the considered widths in the preliminary  
 316 analysis assures that the number of sectors is a natural number between 2  
 317 and 8) by defining the following thresholds:

$$l_j = \alpha_0 + \frac{2j-1}{2} \cdot h, \quad j = 1, \dots, r$$

$$l_0 = l_r$$

318 This procedure provides the definition of  $\mathbf{l}$  and  $r$ , given values of  $\alpha_0$  and  
 319  $h$ . Once the sectors have been defined, AR coefficients can be estimated for  
 320 each regime once more by means of the Yule-Walker equations. Figure 3  
 321 shows the *NRMSE* obtained in the validation-set as a function of  $p$  and  $r$ ,  
 322 when considering the optimal orientation  $\alpha_0$  obtained. It can be noted that

323 the model with the best generalization capability was obtained for the case of  
 324  $p = 3$ . In the same way, it does not seem to be worth increasing the number  
 325 of regimes further than 3. In relation to the orientation sectors, Figure 4  
 326 illustrates the best ones for the six AR(3) models. It can be seen that the  
 327 sectors are placed in such a way that the above mentioned low predictability  
 328 orientation ( $W-NW$ ) tends to form an independent regime, independently of  
 329 the number of regimes considered.

330 The TARSO( $wd$ ) model that showed the best performance in the validation-  
 331 set was:

$$\hat{y}_t = \begin{cases} 0.00 + 1.36 \cdot y_{t-1} - 0.51 \cdot y_{t-2} + 0.14 \cdot y_{t-3}, & s_t = 1 \\ 0.01 + 1.40 \cdot y_{t-1} - 0.54 \cdot y_{t-2} + 0.13 \cdot y_{t-3}, & s_t = 2 \\ 0.00 + 1.19 \cdot y_{t-1} - 0.43 \cdot y_{t-2} + 0.23 \cdot y_{t-3}, & s_t = 3 \end{cases}$$

332 The regimes were given by:

$$s_t = \begin{cases} 1, & wd_{t-1} \in [-41^\circ, 79^\circ) \\ 2, & wd_{t-1} \in [79^\circ, 199^\circ) \\ 3, & wd_{t-1} \in [199^\circ, 319^\circ) \end{cases}$$

#### 333 4.2.3. CPARX models based on a wind direction criterion: CPARX( $wd$ )

334 The description of CPARX models in Subsection 2.4 highlights that the  
 335 crucial point is how to define the coefficients as a function of a certain exoge-  
 336 nous variable. Considering the previous preliminary analysis, a sinus-shaped  
 337 dependence is proposed:

$$\hat{y}_t = \theta_0(wd_{t-1}) + \sum_{i=1}^p \theta_i(wd_{t-1}) \cdot y_{t-i} \quad (15)$$

$$\theta_i(wd_{t-1}) = a_i + b_i \cdot \cos(wd_{t-1} - \phi_0), \quad i = 0, \dots, p \quad (16)$$

338  $a_i$  being the mean level of the  $i$ 'th AR coefficient and  $b_i$  being the amplitude  
 339 of the dependence of  $\theta_i$  on the wind direction. Then, for a given value of  $p$ ,  
 340 the set of parameters is formed by:

$$\Theta_{CPARX} = \{a_0, \dots, a_p, b_0, \dots, b_p, \phi_0\} \quad (17)$$

341  $\Theta_{CPARX}$  is estimated in accordance with Eq. (3). As in the previous case,  
 342 the best performance in the validation-set was achieved for the case of  $p = 3$ .  
 343 Figure 5 collects the AR coefficients for the AR model, the TARSO( $wd$ )  
 344 model and the CPARX( $wd$ ) model.

#### 345 4.3. Modelling the influence of the local wind speed

346 Following a similar methodology, this subsection focuses on how the local  
 347 wind speed can be used to define regimes or smooth dependences in the wind  
 348 power time series dynamics. A preliminary analysis between the predicted  
 349 variable and the wind speed is firstly performed. Then, the TARSO( $ws$ )  
 350 model and the CPARX( $ws$ ) model are obtained.

##### 351 4.3.1. Preliminary analysis

352 Let us consider the interval of wind speeds  $I = [ws_0 - h/2, ws_0 + h/2)$ .  
 353 An AR( $p$ ) model is trained taking into account only those data that satisfy  
 354 at time  $t$  the condition  $ws_{t-1} \in I$ . For a certain  $h$ , the AR coefficients and  
 355 the  $NRMSE$  obtained are related to the wind speed  $ws_0$ . Then, the interval

356  $I$  slides over the spanned space of the wind speed in order to reveal how  
 357 the time series dynamic and the predictability vary with  $ws_0$ . The following  
 358 conclusions were obtained, where the considered values for  $p$  ranged from 1  
 359 to 5: (i) The AR coefficients show a certain dependence on the wind speed.  
 360 This dependence is close to be linear in a substantial part of the wind speed  
 361 range, as is shown in the Figure 6 (case  $p = 2$ ,  $h = 4$  m/s). (ii) The *NRMSE*  
 362 tends to be higher for high wind speeds, showing a maximum at a wind speed  
 363 of around 10 – 12 m/s. However, a decrease in the *NRMSE* is observed for  
 364 wind speeds beyond the nominal wind speed (at which the output power  
 365 is constant up to the cut-off wind speed). (iii) A similar tendency of the  
 366 relationship between *NRMSE* and wind speed has been found for both the  
 367 training-set and the validation-set (see Figure 6). This fact suggests that  
 368 the data sets are representative enough to consider this information valid for  
 369 future time periods.

#### 370 4.3.2. *TARSO* models based on a wind speed criterion: *TARSO(ws)*

371 The prior analysis reveals that a regime-switching model can be imple-  
 372 mented in order to catch different predictability levels, though a low regimes  
 373 number is suggested from Figure 6. In this case, the optimisation process  
 374 considers the threshold values,  $\mathbf{l}$ , as parameters to be estimated. Then, for a  
 375 certain number of regimes,  $r$ , and the AR order  $p$ , the set of parameters to  
 376 estimate is given by:

$$\Theta_{TARSO} = \{\Theta_{AR^{(1)}}, \dots, \Theta_{AR^{(r)}}, \mathbf{l}\} \quad (18)$$

377  $\Theta_{TARSO}$  is estimated by means of a numerical algorithm based on the  
 378 criterion given by Eq. (3). Two and three regimes have been proposed

379 with AR orders going from 1 to 5. In all the cases, the  $AR(3)$  showed  
 380 the best performance in the validation-set (see Figure 7). Furthermore, the  
 381 two-regimes model was slightly better than the three-regimes one. Figure 8  
 382 illustrates the power curve depicted under the optimised regimes. In both  
 383 cases, the thresholds obtained seems to be related to the shape of the power  
 384 curve. First, considering two regimes lead to a threshold of around 10  $m/s$   
 385 near the inflexion point. This value splits up the power curve in two regions:  
 386 (i) the first one is characterized by a convex relationship between the wind  
 387 speed and the output power. In an ideal case, this relationship is a cubic  
 388 polynomial given by  $P = \frac{1}{2}\rho C_p A v^3$ , where  $\rho$  is the density of air,  $C_p$  is the  
 389 power coefficient,  $A$  is the area swept by the rotor blades and  $v$  is the wind  
 390 speed. (ii) The second part is characterized by a concave relationship, since  
 391 the output power has to be limited by the rated power of the wind turbine.  
 392 On the other hand, considering three regimes leads to a division clearly based  
 393 on the slope of the power curve: two regimes for the two flat regions (for low  
 394 and high wind speeds) and a third one for the steep part.

395 The TARSO( $ws$ ) model with best generalisation capabilities was:

$$\hat{y}_t = \begin{cases} 0.00 + 1.33 \cdot y_{t-1} - 0.50 \cdot y_{t-2} + 0.18 \cdot y_{t-3}, & s_t = 1 \\ -0.02 + 1.22 \cdot y_{t-1} - 0.39 \cdot y_{t-2} + 0.18 \cdot y_{t-3}, & s_t = 2 \end{cases}$$

396 The regimes were given by:

$$s_t = \begin{cases} 1, & ws_{t-1} < 10.08 \\ 2, & ws_{t-1} \geq 10.08 \end{cases}$$

397 *4.3.3. CPARX models based on a wind speed criterion: CPARX(ws)*

398 In this case, a linear dependence between AR coefficients and the last  
 399 available data of wind speed  $ws_{t-1}$  is proposed (Eqs. (19) and (20)). This is  
 400 partially supported by the preliminary analysis: even though this hypothesis  
 401 does not seem to be accurate for low and high wind speeds, Figure 6 reveals  
 402 that it is the case for a substantial part of the wind speed range.

$$\hat{y}_t = \theta_0(ws_{t-1}) + \sum_{i=1}^p \theta_i(ws_{t-1}) \cdot y_{t-i} \quad (19)$$

$$\theta_i(ws_{t-1}) = a_i + b_i \cdot (ws_{t-1}), \quad i = 0, \dots, p \quad (20)$$

403  $a_i$  being the  $i$ 'th AR coefficient at null wind speed and  $b_i$  being the slope of  
 404 the dependence of  $\theta_i$  on the wind speed. The set of parameters is now given  
 405 by  $\Theta_{CPARX} = \{a_0, \dots, a_p, b_0, \dots, b_p\}$  and estimated in accordance with Eq.  
 406 (3). The minimisation process has been carried out for several AR orders,  
 407  $p = 1, 2, \dots, 5$ , giving  $p = 3$  the optimal value in terms of generalisation  
 408 capabilities. Figure 9 collects the AR coefficients obtained as a function of the  
 409 wind speed for the AR model, the TARSO( $ws$ ) model and the CPARX( $ws$ )  
 410 model.

411 *4.4. Combining both effects: CPARX(wd,ws)*

412 Results concerning the incorporation of local wind direction and local  
 413 wind speed in varying-coefficient models will be discussed in Section 5. How-  
 414 ever, at this point, it is worth noting that CPARX models showed a better  
 415 performance than TARSO models when modelling the effect of the considered  
 416 explanatory variable (see Figure 11). Additionally, each exogenous variable

417 seems to provide information about different effects. In base of this hypoth-  
 418 esis, the following CPARX model considering both wind speed and wind  
 419 direction is proposed:

$$\hat{y}_t = \theta_0(wd_{t-1}, ws_{t-1}) + \sum_{i=1}^p \theta_i(wd_{t-1}, wd_{t-1}) \cdot y_{t-i} \quad (21)$$

420

$$\begin{aligned} \theta_i(wd_{t-1}, ws_{t-1}) &= a_i + b_i \cdot \cos(wd_{t-1} - \phi_0) \\ &+ c_i \cdot (ws_{t-1}), \quad i = 0, \dots, p \end{aligned} \quad (22)$$

421 The set of parameters to be estimated is  $\Theta_{CPARX} = \{a_0, \dots, a_p, b_0, \dots, b_p, c_0, \dots, c_p, \phi_0\}$ .  
 422 In this case, the best model obtained was for an AR order of  $p = 4$ . The  
 423 coefficient-functions  $\theta_i(wd_{t-1}, ws_{t-1})$  are now surfaces that replicates the  
 424 same trends found in the previous sections. As an example, the case of  
 425  $\theta_1$  is illustrated in Figure 10.

## 426 5. Results

427 This section gathers the results obtained over the test-set, when the op-  
 428 timal parametrisation of each model obtained in Section 4 is considered.

429 Globally, the improvements over Persistence ranged from almost 4% to  
 430 more than 5.5% (see Fig. 11). This represents a good performance, since Per-  
 431 sistence is traditionally difficult to improve on for a prediction horizon of 10  
 432 minutes. With regard to the reference models and in accordance with the pre-  
 433 vious studies [29, 30], improvements in very-short term point-forecasting can  
 434 be attained when considering several regimes under the absence of other ex-  
 435 planatory variables. In particular, MSAR models were able to capture shifts  
 436 between non-observed meteorological states, delivering information about



437 wind power fluctuations and providing a better performance than Persistence  
438 and linear AR models.

439 The models taking into account exogenous variables overcome the refer-  
440 ence models. Regarding the influence of the local wind direction, a similar  
441 relationship between this variable and the AR parameters was identified by  
442 the TARSO( $wd$ ) and the CPARX( $wd$ ) models, as shown in Figure 5. In par-  
443 ticular, given that Persistence can be considered as a particular case of AR  
444 model with  $\theta_1 = 1$  and  $\theta_i = 0, \forall i > 1$ , both TARSO( $wd$ ) and CPARX( $wd$ )  
445 models were likely to become globally closer to Persistence for wind direc-  
446 tions related to the W-NW sector, characterized by a low predictability (the  
447 only exception being  $\theta_3$ , which experiences a small increment for the men-  
448 tioned wind directions). Additionally, a smooth dependence of the wind  
449 power dynamics on the local wind direction was found to be preferable to  
450 considering different regimes (though special attention was paid to track the  
451 optimal number of sectors and their orientation) given the  $IoP$  of 4.98% and  
452 4.66% respectively. Similar conclusions were obtained when the local wind  
453 speed was considered as an exogenous variable: both models TARSO( $ws$ )  
454 and CPARX( $ws$ ) became globally closer to Persistence (with the only ex-  
455 ception of  $\theta_3$ , which remains almost constant) for high wind speeds (Figure  
456 9) characterized by a lower predictability, and a smooth dependence of the  
457 coefficient-functions on the wind speed provided a better result than the  
458 regime-switching strategy (an  $IoP$  of 4.82% compared to 4.58%).

459 In general, the models that took into account the wind direction at-  
460 tained slightly better results than those including the wind speed. This  
461 was also found when considering the results depicted monthly (Tables 2 and

3), the only exception being the month of January. However, in both a globally and a monthly basis, the best performance was clearly attained by the CPARX( $wd,ws$ ). This model attained a global  $IoP$  of 5.72%, which represents almost the addition of the single improvements obtained by the CPARX( $wd$ ) and the CPARX( $ws$ ) models with respect to the AR model. This finding is particularly significant as it supports the notion that each explanatory variable gives information about effects of a different nature.

### 5.1. Further discussion

It was found that the incorporation of the wind direction as an explanatory variable leads to an appreciable improvement of the prediction performance. It could be due to the fact that the proposed models managed to capture some influence of the local wind direction on the wind power time series dynamics. Vincent et al. [42] related the influence of the wind direction on the wind variability at Horns Rev to synoptic scale forcings combined with the location of the wind farm with respect to the shore. In particular, a high wind variability was observed for Westerly winds. According to Akhmatov [47], the implementation of the models of Subsection 4.2 evidences that these effects are propagated to the wind power time series. As mentioned above, it is interesting to note that a smooth dependence of the wind power dynamics on the local wind direction was preferable to a regime switching strategy. This could be explained by taking the following considerations: the present study is focused on an offshore wind farm, characterized by a flat topography with a uniform-clustered distribution of the wind turbines over a squared area. Hence, for this wind farm configuration no obstacle is introducing directional aerodynamic disturbances and, additionally, wind turbine

487 wakes are likely to have a weaker impact on the dependence between the wind  
488 power and the local wind direction compared to the case of a single row wind  
489 farm configuration. Even though some works [10, 11] suggest a considerable  
490 influence of the wakes for very narrow sectors around the wind turbines line  
491 direction, this seems to be too specific to be relevant from a statistical point  
492 of view (at least with the models considered in this work). Our results suggest  
493 that the influence of the local wind direction on the wind power dynamics  
494 was likely to be related to synoptic conditions rather than microscale effects.  
495 However, microscale effect could become predominant in other study cases.  
496 Modelling the influence of the local wind direction in wind farms located in  
497 complex terrain, where topographic obstacles and non-homogeneity of the  
498 terrain introduce strong directional dependences on the power production,  
499 could require other AR coefficient-functions, instead of the sinus-shaped ones  
500 proposed here. Furthermore, wind farms with a non-squared distribution of  
501 wind turbines, for instance row-configured wind farms, could even require a  
502 regime switching strategy, since the wind turbine wakes would affect dramat-  
503 ically the performance of the wind farm for certain wind directions. In any  
504 case, further research on complex terrain and different configuration of wind  
505 farms would be required for confirmation.

506       On the other hand, when the local wind speed was considered as an exoge-  
507 nous variable, the optimisation of the models were likely to be related to the  
508 characteristics of the non-linear power transformation process. Considering  
509 that the power curve represents a non-linear transformation from wind speed  
510 to wind power, the slope of this curve provokes an amplification/reduction  
511 effect of the wind speed fluctuations. It has a direct impact on the out-

512 put power dynamics, causing a dependence between the wind speed and the  
513 predictability of the output wind power. Hence, the improvement obtained  
514 could be due to the fact that the wind speed was employed as a signal about  
515 this non-linear effect. The regime-switching strategy provided thresholds of  
516 wind speed that divide the power curve into particular parts (convex-concave  
517 for the case of 2 regimes and low-high-low amplification level for the case of  
518 3 regimes, see Figure 8). For the case of the conditional parametric model,  
519 a linear relationship between the AR coefficients and the wind speed seemed  
520 to be appropriate for a greater part of the wind speed range. However, the  
521 saturation effect of the output power related to extreme wind speeds (close  
522 to zero or above the nominal wind speed) has not been addressed. Future  
523 work could deal with this topic by considering the Generalized Logit trans-  
524 formation described in Pinson [48] or the so-called ‘break-point models’, a  
525 special subclass of varying-coefficient models that combine both CPARX and  
526 TARSO models (see the closing discussion in Hastie and Tibshirani [49]).

## 527 **6. Conclusions**

528 We have presented a study focused on modelling the influence of local  
529 wind speed and direction on the dynamics of a wind power time series. With  
530 this purpose, a benchmark between several varying-coefficient models for 10  
531 minute-ahead forecasting was carried out. The models are built by general-  
532 ising the conventional linear AR structure, following two approaches: regime  
533 switching models and conditional parametric models. By comparing the ac-  
534 curacy of the models, findings about the most suitable statistical approach  
535 were also obtained.

536 It was found that local measurements of both wind speed and direction  
537 provide useful information for a better comprehension of the wind power time  
538 series dynamics, at least when considering the case of the very-short term  
539 forecasting. In particular, the results suggest that different effects can be  
540 modelled depending on the considered explanatory variable: the local wind  
541 direction contributes to model some features of the prevailing winds, such as  
542 the impact of the wind direction on the wind variability, whereas the non-  
543 linearities related to the power transformation process can be introduced  
544 by considering the local wind speed. Additionally, for our particular case  
545 study, it was found that the conditional parametric models outperforms a  
546 regime-switching strategy.

547 It is interesting to note that the influence of both local wind speed and  
548 direction were modelled under the assumption of observable processes, and  
549 that only the last observation was taken into account. This study highlights  
550 two main lines for further research: the first one is to consider non-observable  
551 processes based on local observations, by incorporating exogenous variables  
552 whether in the transition matrix or in the definition of the AR coefficients  
553 of MSAR models. The second one is to include previous lags of the local  
554 observations in order to get a model sensitive to the evolution of the con-  
555 sidered exogenous variable. By doing this, it would be possible to explore  
556 new effects that condition the dynamics of the output wind power time series  
557 (e.g. abrupt changes in local wind direction related to certain meteorological  
558 conditions).

559 Finally, the models here presented could be upgraded by letting the co-  
560 efficients vary smoothly with time so as to capture seasonal variabilities of

561 wind power dynamics due to climatological effects and the decrease of the  
562 wind turbine performance.

## 563 **7. Acknowledgements**

564 Acknowledgements are first due to CIEMAT who is founding the research  
565 of the first author through its PhD Scholarship Program. The work presented  
566 has also been partly supported by the Danish ForskEL programme through  
567 the project “Radar@Sea” (ForskEL 2009-1-0226) and the project “Mesoscale  
568 atmospheric variability and the variation of wind and production for offshore  
569 wind farms”, sponsored by the Danish Public Service Obligation (PSO) fund  
570 (PSO 7141), which are hereby acknowledged. We are thankful to Vattenfall  
571 Denmark for originally providing the wind and power measurements for the  
572 Horns Rev wind farm, and to Pierre-Julien Trombe for the data processing  
573 and quality checking.

## 574 **References**

- 575 [1] Purvins A, Zubaryeva A, Llorente M, Tzimas E, Mercier A. Challenges  
576 and options for a large wind power uptake by the European electricity  
577 system. *Applied Energy* 2011;88(5):1461–9.
- 578 [2] Snyder B, Kaiser MJ. A comparison of offshore wind power development  
579 in europe and the U.S.: Patterns and drivers of development. *Applied*  
580 *Energy* 2009;86(10):1845–56.
- 581 [3] Giebel G. The state of the art in short-term prediction of wind power -  
582 A literature overview. Tech. Rep.; ANEMOS EU project; 2003.

- 583 [4] Landberg L, Giebel G, Nielsen H, Nielsen T, Madsen H. Short-term  
584 prediction - An overview. *Wind Energy* 2003;6(3):273–80.
- 585 [5] Costa A, Crespo A, Navarro J, Lizcano G, Madsen H, Feitosa E. A  
586 review on the young history of the wind power short-term prediction.  
587 *Renewable and Sustainable Energy Reviews* 2008;12(6):1725–44.
- 588 [6] Pinson P, Nielsen H, Madsen H, Kariniotakis G. Skill forecasting from  
589 ensemble predictions of wind power. *Applied Energy* 2009;86(7-8):1326–  
590 34.
- 591 [7] Bouzgou H, Benoudjit N. Multiple architecture system for wind speed  
592 prediction. *Applied Energy* 2011;88(7):2463–71.
- 593 [8] Costa A. Mathematical/statistical and physical/meteorological models  
594 for short-term prediction of wind farms output. Ph.D. thesis; Escuela  
595 Técnica Superior de Ingenieros Industriales (Universidad Politécnica de  
596 Madrid); 2005.
- 597 [9] Orlanski I. A rational subdivision of scales for atmospheric processes.  
598 *Bulletin of the American Meteorological Society* 1975;56:527–30.
- 599 [10] Jensen L, Mørch C, Sørensen PB, Svendsen KH. Wake measurements  
600 from the Horns Rev off-shore wind farm. *European Wind Energy Con-*  
601 *ference, London; 2004.*
- 602 [11] Méchali M, Barthelmie R, Frandsen S, Jensen L, Réthoré PE. Wake  
603 effects at Horns Rev and their influence on energy production. *European*  
604 *Wind Energy Conference, Greece; 2006.*

- 605 [12] Brown B, Katz R, Murphy A. Time series models to simulate and  
606 forecast wind speed and wind power. *Journal of Climate and Applied*  
607 *Meteorology* 1984;23(8):1184–95.
- 608 [13] Huang Z, Chalabi ZS. Use of time-series analysis to model and forecast  
609 wind speed. *Journal of Wind Engineering and Industrial Aerodynamics*  
610 1995;56(2-3):311–22.
- 611 [14] Kennedy S, Rogers P. A probabilistic model for simulating long-term  
612 wind-power output. *Wind Engineering* 2003;27(3):167–81.
- 613 [15] Torres J, Garcia A, De Blas M, De Francisco A. Forecast of hourly av-  
614 erage wind speed with ARMA models in Navarre (Spain). *Solar Energy*  
615 2005;79(1):65–77.
- 616 [16] De Giorgi MG, Ficarella A, Tarantino M. Error analysis of short term  
617 wind power prediction models. *Applied Energy* 2011;88(4):1298–311.
- 618 [17] Erdem E, Shi J. ARMA based approaches for forecasting the tuple of  
619 wind speed and direction. *Applied Energy* 2011;88(4):1405–14.
- 620 [18] Liu H, Erdem E, Shi J. Comprehensive evaluation of ARMA-GARCH(-  
621 M) approaches for modeling the mean and volatility of wind speed. *Ap-  
622 plied Energy* 2011;88(3):724–32.
- 623 [19] Li G, Shi J. On comparing three artificial neural networks for wind  
624 speed forecasting. *Applied Energy* 2010;87(7):2313–20.
- 625 [20] Cleveland WS, Grosse E, Shyu WM. *Statistical models in S*; chap.



- 626 Local regression models. Boca Raton, FL, USA: CRC Press, Inc. ISBN  
627 0412052911; 1991, p. 309–76.
- 628 [21] Tong H. Threshold models in non-linear time series analysis. Springer-  
629 Verlag; 1983.
- 630 [22] Gneiting T, Larson K, Westrick K, Genton MG, Aldrich E. Calibrated  
631 probabilistic forecasting at the stateline wind energy center: The regime-  
632 switching space-time method. *Journal of the American Statistical As-  
633 sociation* 2006;101(475):968–79.
- 634 [23] Tastu J, Pinson P, Kotwa E, Madsen H, Nielsen HA. Spatio-temporal  
635 modelling of short-term wind power prediction errors. *Wind Energy*  
636 2011;14(1):43–60.
- 637 [24] Hering AS, Genton MG. Powering up with space-time wind forecasting.  
638 *Journal of the American Statistical Association* 2010;105(489):92–104.
- 639 [25] Castino F, Festa R, Ratto C. Stochastic modelling of wind velocities  
640 time series. *Journal of Wind Engineering and Industrial Aerodynam-  
641 ics* 1998;74-6:141–51. 2nd European and African Conference on Wind  
642 Engineering, Genoa, Italy, Jun 22-26, 1997.
- 643 [26] Hughes JP, Guttorp P, Charles SP. A non-homogeneous Hidden Markov  
644 Model for precipitation occurrence. *Journal of The Royal Statistical  
645 Society Series C* 1999;48(1):15–30.
- 646 [27] Ailliot P. Modèles autorégressifs à changements de régimes markoviens.  
647 Applications aux séries temporelles de vent. Ph.D. thesis; University of  
648 Rennes; 2004.

- 649 [28] Kosater P, Mosler K. Can Markov regime-switching models improve  
650 power-price forecasts? Evidence from German daily power prices. *Ap-  
651 plied Energy* 2006;83(9):943–58.
- 652 [29] Pinson P, Christensen LEA, Madsen H, Sørensen PE, Donovan MH,  
653 Jensen LE. Regime-switching modelling of the fluctuations of offshore  
654 wind generation. *Journal of Wind Engineering and Industrial Aerody-  
655 namics* 2008;96(12):2327–47.
- 656 [30] Pinson P, Madsen H. Adaptive modeling and forecasting of wind power  
657 fluctuations with Markov-switching autoregressive models. *Journal of  
658 Forecasting* 2010;in press.
- 659 [31] Chen R, Tsay RS. Functional-coefficient Autoregressive models. *Journal  
660 of the American Statistical Association* 1993;88(421):298–308.
- 661 [32] Nielsen HA, Nielsen TS, Joensen AK, Madsen H, Holst J. Tracking time-  
662 varying-coefficient functions. *International Journal of Adaptive Control  
663 and Signal Processing* 2000;14(8):813–28.
- 664 [33] Sánchez I. Short-term prediction of wind energy production. *Interna-  
665 tional Journal of Forecasting* 2006;22(1):43–56.
- 666 [34] Fan J, Zhang W. Statistical methods with varying-coefficient models.  
667 *Statistics and its Interface* 2008;1:179–95.
- 668 [35] Cleveland WS, Devlin SJ. Locally-weighted regression: an approach to  
669 regression analysis by local fitting. *Journal of the American Statistical  
670 Association* 1988;83:596–610.

- 671 [36] Nielsen T, Madsen H, Nielsen H. Prediction of wind power using  
672 time-varying coefficient-functions. Proceedings of the 15th IFAC World  
673 Congress on Automatic Control, Barcelona (Spain); 2002.
- 674 [37] Madsen H, Pinson P, Kariniotakis G, Nielsen HA, S.Nielsen T. Stan-  
675 dardizing the performance evaluation of short-term wind power predic-  
676 tion models. *Wind Engineering* 2005;29(6):475–89.
- 677 [38] Hamilton JD. A new approach to the economic analysis of nonstationary  
678 time series and the business cycle. *Econometrica* 1989;57(2):357–84.
- 679 [39] Krolzig HM. Markov-switching vector autoregressions. Springer; 1997.
- 680 [40] Nielsen HA, Nielsen TS, Madsen H. ARX-models with parameter varia-  
681 tions estimated by local fitting. In: Sawaragi Y, Sagara S, editors. 11th  
682 IFAC Symposium on System Identification; vol. 2. 1997, p. 475–80.
- 683 [41] Madsen H, Holst J. Modelling non-linear and non-stationary time series.  
684 Technical University of Denmark, DTU Informatics; 2000.
- 685 [42] Vincent CL, Pinson P, Giebel G. Wind fluctuations over the North Sea.  
686 *International Journal of Climatology* 2010;in press.
- 687 [43] Peña D. Estadística. Modelos y métodos; vol. 2. Alianza Editorial; 2nd  
688 ed.; 1987.
- 689 [44] Dempster AP, Laird NM, Rubin DB. Maximum likelihood from in-  
690 complete data via the EM algorithm. *Journal of the Royal Statistical*  
691 *Society, Series B* 1977;39(1):1–38.

- 692 [45] Hamilton JD. Analysis of time series subject to changes in regime.  
693 Journal of Econometrics 1990;45(1-2):39–70.
- 694 [46] Patterson DM. Nonlinear time series analysis of economic and financial  
695 data; chap. A markov switching cookbook. Kluwer Academic; 1999, p.  
696 33–43.
- 697 [47] Akhmatov V. Influence of wind direction on intense power fluctua-  
698 tions in large offshore windfarms in the North Sea. Wind Engineering  
699 2007;31(1):59–64.
- 700 [48] Pinson P. On probabilistic forecasting of wind power time-series. Tech.  
701 Rep.; Technical University of Denmark, DTU Informatics; 2010.
- 702 [49] Hastie T, Tibshirani R. Varying-coefficient models. Journal of the Royal  
703 Statistical Society, Series B (Methodological) 1993;55(4):757–96.

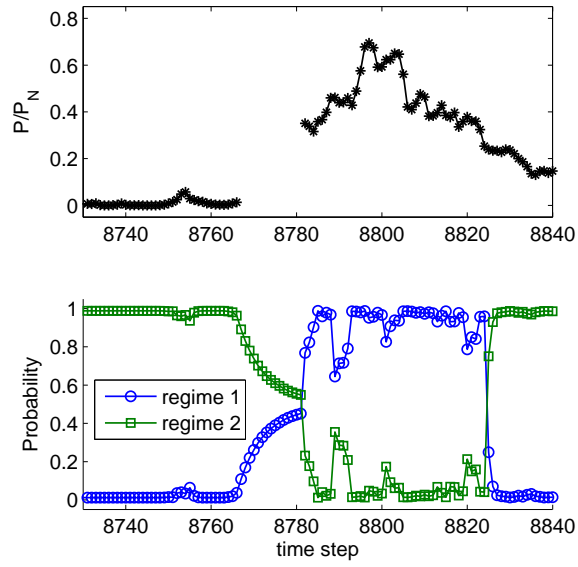


Figure 1: Filtered probabilities of the current regime provided by the MSAR model during periods with missing data.  $P/P_N$  represents the output power ( $P$ ) normalized with the rated power of the wind farm ( $P_N$ ).

704  
 705  
 706  
 707  
 708  
 709  
 710  
 711  
 712  
 713

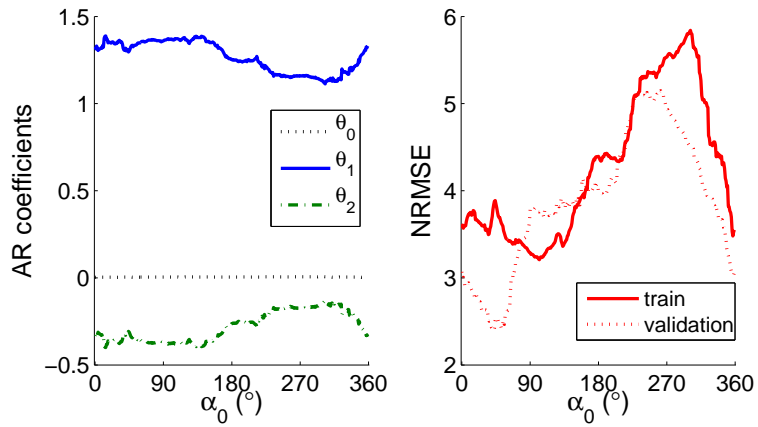


Figure 2: Dependence of the AR coefficients (left) and  $NRMSE$  in  $\%P_N$  (right) with local wind direction. Case for AR order  $p = 2$

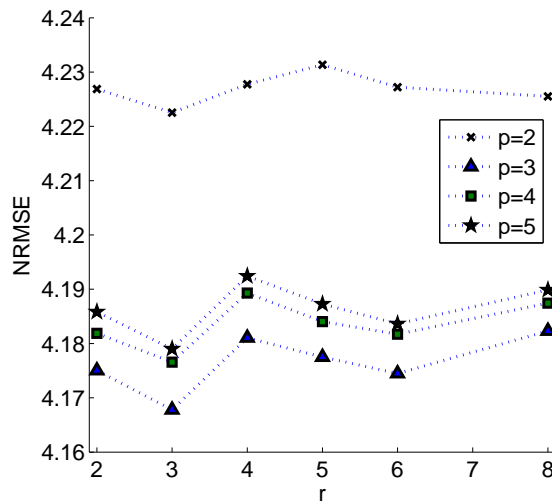


Figure 3:  $NRMSE$  (in  $\%P_N$ ) of  $TARSO(wd)$  over the validation-set, as a function of the number of regimes,  $r$ , and the AR order,  $p$ . Results for  $p = 1$ , layout of the picture due to a higher  $NRMSE$

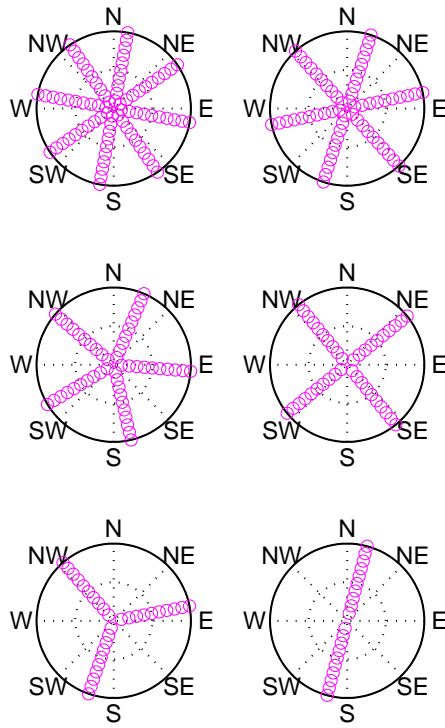


Figure 4: Optimal orientation of the sectors depending on the number of regimes considered in a TARSO( $wd$ ) model, case for AR order  $p = 3$

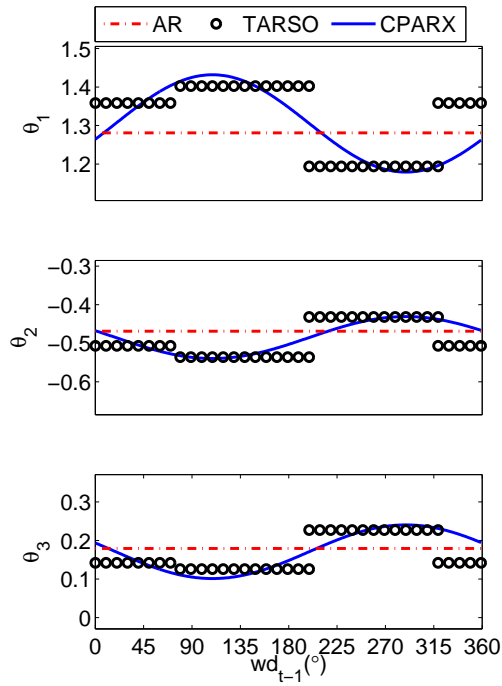


Figure 5: Dependence of the AR coefficients with local wind direction for AR, TARSO( $wd$ ) and CPARX( $wd$ ) models ( $\Theta_0$  is omitted, since it is very close to zero for every model)



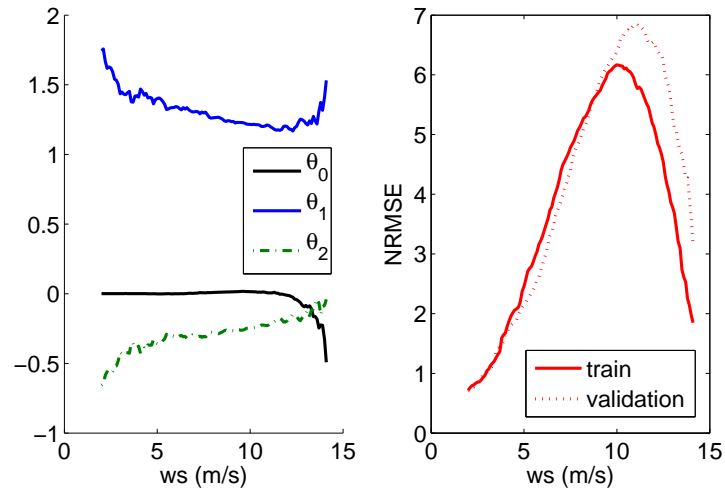


Figure 6: Dependence of the AR coefficients and  $NRMSE$  (in  $\%P_N$ ) with local wind speed. Case for AR order  $p = 2$

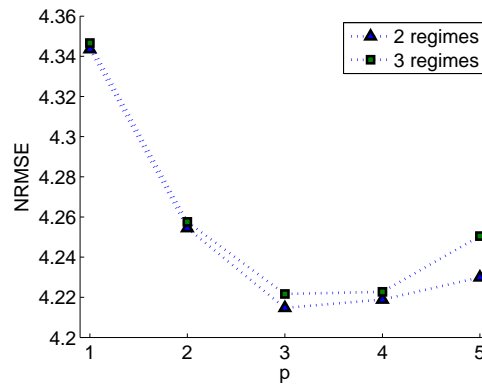


Figure 7:  $NRMSE$  (in  $\%P_N$ ) of  $TARSO(ws)$  over the validation-set, as a function of the number of regimes,  $r$ , and the AR order,  $p$

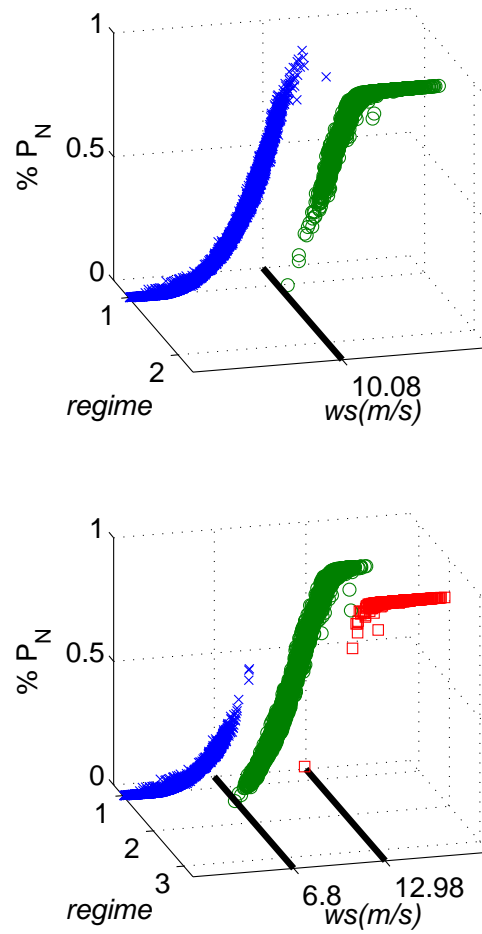


Figure 8: Optimal splitting of the power curve for TARSO( $ws$ ) models

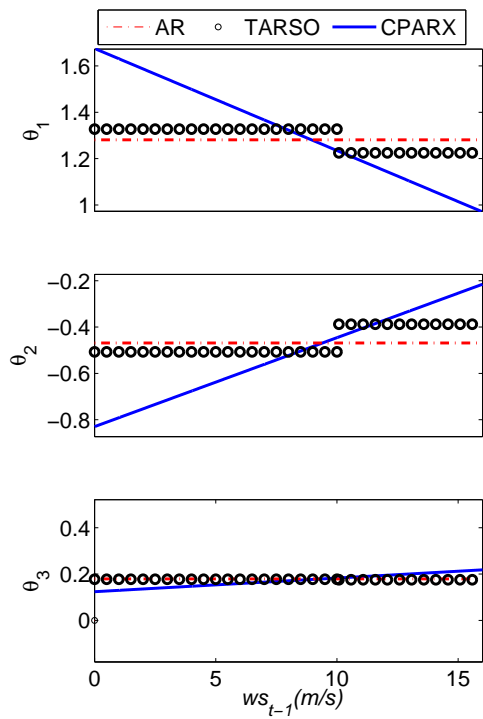


Figure 9: Dependence of the AR coefficients for AR, TARSO( $ws$ ) and CPARX( $ws$ ) models. ( $\Theta_0$  is omitted, since it is very close to zero for every model)

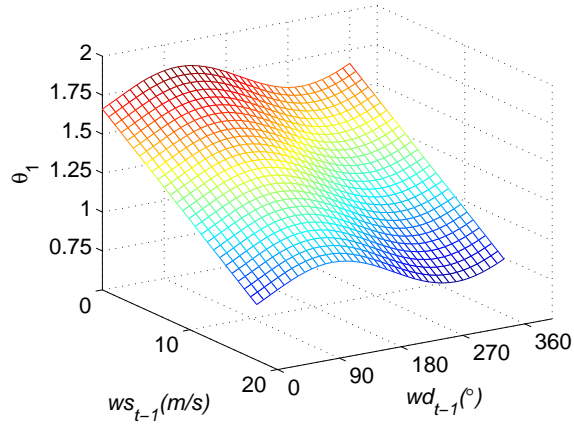


Figure 10:  $\theta_1$  as a function of local wind direction and local wind speed for the  $CPARX(wd,ws)$  model

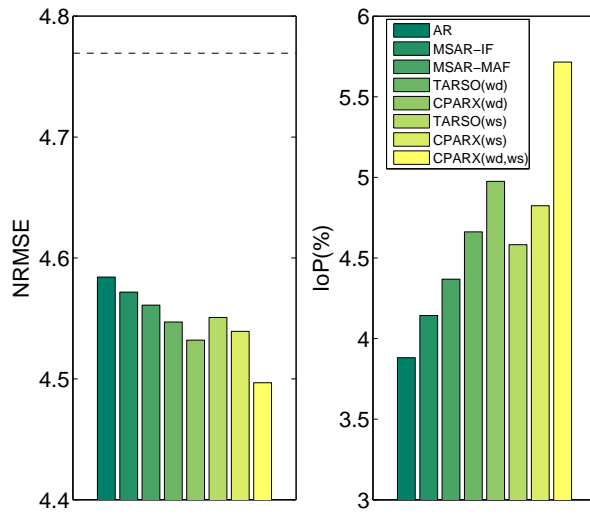


Figure 11:  $NRMSE$  (in  $\%P_N$ ) and  $IoP$  for the test-set. Dashed line of the figure on the left refers to the  $NRMSE$  of Persistence

Constant coefficients	
	<b>Persistence</b> <sup>1,2,3</sup> , <b>AR</b> <sup>2,3,4</sup> , <b>ARMA</b> <sup>1,5,6</sup>
Varying coefficients	
R-S (Obs)	STAR <sup>1</sup> , SETAR <sup>1</sup> , <b>TARSO</b> <sup>7</sup>
R-S (Non-Obs)	<b>MSAR</b> <sup>1,2,8</sup>
C-P	<b>CPARX</b> <sup>3,9</sup>

Table 1: Summary of models applied in some studies related to short-term wind and wind power forecasting. In bold, models considered in the present study. **R-S**: Regime-Switching, **C-P**: conditional parametric, **Obs**: Observable process. <sup>1</sup>Pinson et al. [29], <sup>2</sup>Pinson and Madsen [30], <sup>3</sup>Pinson [48], <sup>4</sup>Brown et al. [12], <sup>5</sup>De Giorgi et al. [16], <sup>6</sup>Erdem and Shi [17] <sup>7</sup>Tastu et al. [23], <sup>8</sup>Ailliot [27], <sup>9</sup>Nielsen et al. [36]

	September	October	November	December	January
Persistence	4.66	4.16	6.25	4.76	4.07
AR	4.44	3.96	6.03	4.42	3.98
MSAR-IF	4.43	3.95	5.97	4.47	3.97
MSAR-MAF	4.41	3.96	5.95	4.41	4.00
TARSO( <i>wd</i> )	4.42	<b>3.92</b>	5.94	4.37	3.99
CPARX( <i>wd</i> )	<b>4.41</b>	3.92	<b>5.91</b>	<b>4.37</b>	3.97
TARSO( <i>ws</i> )	4.44	3.93	5.94	4.39	3.97
CPARX( <i>ws</i> )	4.42	3.94	5.92	4.37	<b>3.94</b>
CPARX( <i>wd,ws</i> )	<b>4.41</b>	<b>3.91</b>	<b>5.82</b>	<b>4.35</b>	<b>3.93</b>

Table 2: *NRMSE* depicted monthly. The two lowest values in each column are given in bold fonts. The overall results are gathered in Figure 11

	September	October	November	December	January
AR	4.73	4.89	3.54	7.19	2.33
MSAR-IF	4.74	5.04	4.43	6.10	2.50
MSAR-MAF	5.30	4.81	4.80	7.46	1.80
TARSO( <i>wd</i> )	5.07	<b>5.72</b>	4.87	8.17	2.07
CPARX( <i>wd</i> )	<b>5.34</b>	5.71	<b>5.41</b>	<b>8.34</b>	2.54
TARSO( <i>ws</i> )	4.72	5.65	4.89	7.89	2.57
CPARX( <i>ws</i> )	5.07	5.39	5.16	8.14	<b>3.30</b>
CPARX( <i>wd,ws</i> )	<b>5.37</b>	<b>5.96</b>	<b>6.78</b>	<b>8.68</b>	<b>3.54</b>

Table 3: *IoP* depicted monthly. The two highest values in each column are given in bold fonts. The overall results are gathered in Figure 11